Discontinuities in the solar wind and its implication to the transport of energetic particles

Gang Li *

* *Department of Physics and CSPAR, University of Alabama, Huntsville, AL 35899, USA*

***Abstract*. Solar wind plasma is an ideal site for studying the property of Magnetohydrodynamic (MHD) turbulence. At small scales, solar wind is believed to be very multi-fractal with nonlinear interactions causing an intermittent energy dissipation, leading to coherent structures that often manifest them as discontinuities. One of the most common coherent structures is current sheet. A current sheet is a structure upon crossing of which the magnetic field directions change abruptly. The presence of these structures in the solar wind introduces a new source of MHD turbulence intermittency. It can affect the transport of energetic particles. Here we illustrate a systematic data analysis procedure to examine the existence of current sheets in the solar wind and study the effects of these structure on the transport of energetic particles.**

***Keywords*: Solar wind, current sheet, MHD turbulence, intermittency, particle transport**

I. INTRODUCTION

Solar wind is a collisionless plasma and our best place to study magnetohydrodynamics (MHD) turbulence. Understanding the orgin and the evolution of solar wind MHD turbulence is not only important by itself, but also of great importances to problems such as the transport of energetic particles in the solar wind. For example, the long embraced Parker's transport equation [1] is based on the implicit assumption that the propagation of charged particle in the solar wind can be described by diffusion, in both the parallel and perpendicular direction to the background magnetic field. However, it has been known that if the geometry of the turbulence is of "slab" (i.e. the wave vector is parallel to the background B_0), then the motion of a charged particle in the perpendicular direction is described by subdiffusion [2], [3]. This would cause doubts to the vilidity of Parker's transport equation if one assume the turbulence in the solar wind is mostly Alfvénic (which is of slab geometry). However, as we shall demonstrate, the existence of current sheet (the most common intermittent structure in the solar wind) can effectively alter the motion of a charged particle from subdiffusion to diffusion even if the turbulence is purely Alfvénic, therefore validates the diffusion assumption used in Parker's transport equation.

In the following, we discuss two topics. First we discuss how one can identify current sheet in the solar wind and then we discuss the effects of current sheets on the transport of energetic charged particles.

II. CURRENT SHEETS IN THE SOLAR WIND

A central topic of the solar wind MHD turbulence is its intermittent characteristic. In a collisionless plasma, intermittency arises because the fluctuations of magnetic field and fluid velocity are scale dependent, contrary to that conjectured in the K41 theory [4]. This scale dependence reflects how turbulence is unevenly distributed in space. Mathematically, intermittency describes how a structure function $S_q^p(l)$ varies with the order p. Here $S_q^p(l)$ is the p-th order structure function defined for a physcial quantity q (q can be e.g. $v_{||}$ or B) through,

$$S_q^p(l) =< |q(x) - q(x+l)|^p > \approx l^{\zeta_p}, \qquad (1)$$

where ζ_p is the scaling exponent of $S_q^p(l)$ and is in general a function of p. In the absence of intermittency, $\zeta_p = p/m$ with $m = 3$ ($m = 4$) for normal fluid (magnetofluid) respectively. Any deviation from this linear dependence indicates the presence of intermittency.

Burlaga [5] first studied intermittency in the context of solar wind MHD turbulence. He used Voyager data at various heliocentric distances, and showed that the ζ_p associated with flutuating solar wind speed is not linear with p. This is followed by *Marsch & Liu* [6] who analyzed Helios data in the inner heliosphere and showed that not only intermittency exists in the solar wind, but its strength can also differ much depending on plasma properties: small scales are more intermittent than large scales and slow wind is more intermittent than fast wind. Since then, studies on the intermittent character of solar wind have been widely reported [e.g. [7], [8], [9], [10], [11], [12], [13], [14], [15]].

Identification of intermittency to specific structures in the solar wind has been recently reported by Salem et al. and Li [15], [16]. In the work of Li [16], a detailed procedure is proposed to identify current sheets – the most common intermittent structure in the solar wind.

We illustrate this method here. This method consists of two steps. The first step is a statistical study and the second step can be used to locate the exact locations of individual current sheets.

Define a tensor $R(\zeta)$,

$$R_{\alpha,\beta}(\zeta) =< \hat{b}_\alpha(t)\hat{b}_\beta(t+\zeta) > \qquad (2)$$

where α and β are two Cartesian indices in any orthorgonal coordinal system, for example, the Inertial Heliographic coordiate system (IHS) and $\hat{b} = \vec{B}/B$ is the unit magnetic field vector. Taking the trace of $R(\zeta)$,

one obtains a coordinate independent quantity [17],

$$Tr[R(\zeta)] =< \hat{b}(t) \cdot \hat{b}(t+\zeta) > . \quad (3)$$

Clearly, $Tr[R(\zeta)]$ is the ensemble average of the cosine of the angle between $\hat{b}(t)$ and $\hat{b}(t+\zeta)$. It can be related to the probability density function $f(\theta,\zeta)$ of finding an angle between $\hat{b}(t)$ and $\hat{b}(t+\zeta)$ within θ and $\theta+\delta\theta$ through,

$$< \hat{b}(t) \cdot \hat{b}(t+\zeta) >= \int f(\theta,\zeta) cos\theta d\theta. \quad (4)$$

Using the magnetic field data, $f(\theta,\zeta)$ can be computed through,

$$f(\theta,\zeta)\Delta\theta = \frac{N^{\zeta}(\theta < \theta' < \theta+\Delta\theta)}{N^{\zeta}(0 < \theta' < \pi)}. \quad (5)$$

Here $N^{\zeta}(\theta < \theta' < \theta+\Delta\theta)$ is the number of measurement pairs where the angle between $\hat{b}(t)$ and $\hat{b}(t+\zeta)$ is within the range of $(\theta,\ \theta+\Delta\theta)$ and $N^{\zeta}(0 < \theta' < \pi)$ is the total number of measurements. If the total time period is T and the time resolution of the data is δ, one can show that,

$$N^{\zeta}(0 \le \theta \le \pi) = (T-\zeta)/\delta \approx T/\delta. \quad (6)$$

where we assumed $T >> \zeta$ ($T \sim$ a day and $\zeta \sim$ minutes). Hence $N^{\zeta}(0 \le \theta \le \pi)$ is independent of ζ. Now, define the integrated distribution function $F(\theta,\zeta)$ through,

$$F(\theta,\zeta) = \int_{\theta}^{\pi} d\theta' f(\theta',\zeta) = \frac{N^{\zeta}(\theta < \theta' < \pi)}{N^{\zeta}(0 < \theta' < \pi)}. \quad (7)$$

Clearly $F(\theta,\zeta)$ represents the frequency of having the measured angle larger than θ.

Because the magnetic field direction change abruptly from one side of a current sheet to the other, one can show that the quantity $N^{\zeta}(\theta < \theta' < \pi)$, therefore $F(\theta,\zeta)$ scale linearly with the time separation ζ when θ is larger than some critical angle θ_0, i.e.,

$$F(\theta, N\zeta) \sim NF(\theta,\zeta) \qquad \text{when} \quad \theta > \theta_0. \quad (8)$$

This scaling property is the essence of identifying current sheet in the solar wind. To locate individual current sheet, one can use the following procedure [16]: assuming the spacecraft crosses a current sheet at time $t=T$, then during the period $T-\zeta < t < T$, $\hat{b}(t)$ and $\hat{b}(t+\zeta)$ will lie on opposite sides of the current sheet. So for the majority of the following measurements: $\hat{b}(T-\zeta)\cdot\hat{b}(T)$, $\hat{b}(T-\zeta+\delta)\cdot\hat{b}(T+\delta)$, ..., till $\hat{b}(T-\delta)\cdot\hat{b}(T+\zeta-\delta)$, we expect the resultant angles to be larger than a critical angle θ_0. Of course, by the law of statistics, there will be a small fraction of these θs that are smaller than θ_0. One can now identify the location of the current sheets by searching for a series of measurements of θs that satisfy 1) the length of the series is about ζ, and 2) most θs in the series are larger than θ_0. When such a time series ("target series") is found, the time at the end of the "target series" will correspond to the location of the current sheet. If onsidering again measurements of multiple ζs, then because the starting time of the "target series" is $T-\zeta$ and the ending time is T, the obtained "target series" from using different ζs should exhibit a pattern where the ending times are approximately the same ($\sim T$) and the starting times are ordered by $T-\zeta$. To better visualize the pattern, one can include $t+\zeta$ in the "target series". This inclusion will cause the "target series" to be symmetric with respect to $t=T$, and have a length of 2ζ (from $T-\zeta$ to $T+\zeta$). This symmetric pattern allows an easier identification of T than the original asymmetric pattern. In figure 1, a "symmetric pattern" is shown. Although the uppermost line is broken, the overall pattern from all three lines unambiguously shows that the location of the current sheet is $\sim$ 11538321 seconds.

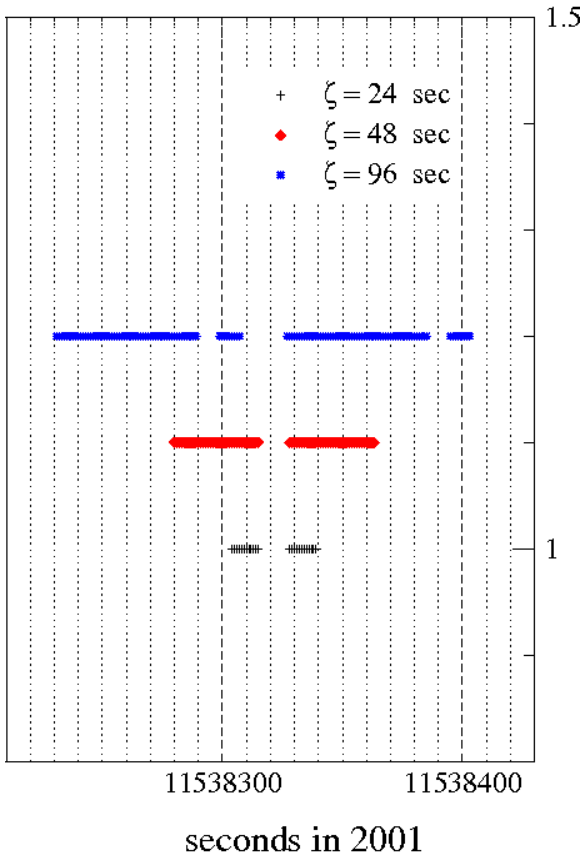

Fig. 1. A current sheet identified during 2001.128 – 2001.154. The center time the pattern gives the location of the current sheet. Adapted from [16].

III. Effects of Current Sheets on Transport of Energetic Particles

We now discuss the effects of flux tubes on the transport of energetic particles. We note that at present the origin of these intermittent structures (i.e. current sheets) are still unknown. It is possible that they have a solar origin as suggested by Borovsky [18]. Alternatively, they may emerge from non-linear interactions in the solar wind [19]. Li *et al.* [20] examined the differences between the solar wind and the Earth's magnetotail using

Cluster and found that current sheets do not exist in the Earth's magnetotail and are unique in the solar wind, suggesting at least a possible solar origin for most of them.

Since the origin of these current sheet is not clear, the author and his co-worker have constructed a phenomenological model of the solar wind in which current sheets are put in by hand. The constructed model is named "cell model" [21]. In the following, we briefly discuss the model and discuss the simulation results.

In this model the solar wind is treated as composed of small cells with random size. In every individual cell, the magnetic field consists of a uniform mean magnetic field B_0^{local}, whose direction may differ from the underlying large scale background field $\vec{B_0}$ but having the same magnitude as $\vec{B_0}$; and a turbulent magnetic field, given by, for example, that of a slab model and/or a 2D turbulence model. We avoid treating detailed plasma properties in our model since we focus on studying the transport of energetic particles. We treat these particles as test particles. We assume the boundaries between cells have no thickness in our model. This "cell model" is a 3D model. The total solar wind occupies a space (denoted as M below) of $100\lambda \times 100\lambda \times 100\lambda$, where λ is the local *intrinsic* turbulence parallel scale. We impose periodic boundary conditions at all six boundary planes. We then divide M into $64^3 = 262144$ convex polyhedron (cells) randomly. The average length scale of the cell l_{cell} is $100\lambda/64$. Taking $\lambda = 0.02$AU as a typical value in the solar wind near 1 AU, we obtain $l_{cell} \sim 0.03$ AU.

Note all lengths are scaled to the local *intrinsic* turbulence correlation scale λ. In each cell, we assume the background magnetic field $\vec{B}_0^{local} = B_0\hat{z}'$. In choosing the direction $\hat{z}'$, we assume the angle between $\hat{z}'$ and $\hat{z}$, $\alpha = cos^{-1}(\hat{z}\cdot\hat{z}')$ obeys the distribution function,

$$F(\alpha) = \frac{2}{\alpha_{max}}\left(1 - \frac{\alpha}{\alpha_{max}}\right), \tag{9}$$

where α_{max} is the maximum angle between $\hat{z}'$ and $\hat{z}$ and taken to be $\alpha_{max} = (5/6)\pi$ in this work. This probability distribution has a maximum at $\hat{z}' = \hat{z}$ and decreases linearly to zero at $\alpha = \alpha_{max}$. Two sets of coordinate systems have been used. The one without primes (x, y, z) denotes Cartesian coordinate with $\hat{z}$ parallel to $\vec{B}^{local}$, and the one with primes (x', y', z') denotes that with $\hat{z}'$ parallel to $\vec{B}^{local}$.

In each cell the total magnetic field $\vec{B}(\vec{x}') = \vec{B}_0^{local} + \vec{b}(\vec{x}')$. Here $\vec{b}$ is a zero-average fluctuation $\vec{b}(\vec{x}')$ and is assumed to be determined with a turbulence model consists of a 1D slab component $\vec{b}^{slab}(z')$ and a 2D component $\vec{b}^{2D}(x', y')$ [1] [22], [23]. We refer to the model turbulence confined in each cell as the local *intrinsic* turbulence, and describe it using numerical methods similar to [3], [24]. We vary the ratio $E^{slab} : E^{total} \equiv E^{slab} : \left(E^{slab} + E^{2D}\right)$ from 0 to 1, to change the turbulence geometry from a pure 2D case to a pure slab case. For the slab component, we take a length of $10,000\lambda$ in the $\hat{z}$ direction and choose a total of $N_z = 2^{22}$ points. For the 2D component, we assume a box with size $10\lambda \times 10\lambda$ and a total of $N_x \times N_y$ points with $N_x = N_y = 4096$.

[1] a 2D geometry is where $\vec{k}$ and δ_B are $\perp B_0$.

The amplitudes for the slab and 2D components are given by,

$$S_{xx}^{slab}(k_\parallel) = \frac{C(\nu)\lambda\langle b_{slab}^2\rangle}{(1 + k_\parallel^2\lambda^2)^\nu}, \tag{10}$$

$$S_{xx}^{2D}(k_\perp) = \frac{C(\nu)\lambda_x\langle b_{2D}^2\rangle}{\pi k_\perp(1 + k_\perp^2\lambda_x^2)^\nu} \tag{11}$$

where the parallel turbulence scale λ is of the order of parallel turbulence correlation length λ_c with $\lambda_c = 2\pi C(\nu)\lambda$, $C(\nu) = (2\pi^{1/2})^{-1}\Gamma(\nu)/\Gamma(\nu - 1/2)$, $\Gamma()$ is the Gamma function and constant $\nu = 5/6$. The perpendicular scale $\lambda_x = 0.1\lambda$ is of the order of perpendicular correlation length.

In studying the effects of the current sheets on the transport of energetic particles, We calculate the running diffusion coefficients using the Kubo formula through,

$$D_x(t) = \langle(\Delta x)^2\rangle/2t \tag{12}$$

$$D_z(t) = \langle(\Delta z)^2\rangle/2t \tag{13}$$

where the brackets $\langle\ldots\rangle$ indicate ensemble average and is calculated by following a total of $10,000,000$ test particles' trajectories using a fourth-order adaptive-step Runge-Kutta method with a relative error control set to 10^{-9} [3], [24]. By varying the ratio of $E^{slab} : E^{total} \equiv E^{slab} : \left(E^{slab} + E^{2D}\right)$ we examine the effect of the local turbulence on both the perpendicular diffusion cefficient $D_x(t)$ and the parallel diffusion coefficient $D_z(t)$.

Figure 2 is interesting. It plots the perpendicular (upper panel) and the parallel (lower panel) running diffusion coefficients when the local *intrinsic* turbulence is of pure slab ($E^{slab} : E^{total} = 1$). The ratio of gyroradius to parallel turbulence correlation length is taken to be $r_L/\lambda_c = 0.097$ and the turbulence level is set to be $b/B_0 = 1$. The thick lines are for the cell model, with current sheets in the solar wind, and the thin lines assume no flux tubes in the solar wind. The dotted line in the upper panel of figure 2 is proportional to $t^{-1/2}$. What is interesting is that in the upper panel, we find that the running perpendicular diffusion coefficients for the case of no cell structure and the case of having cell structure are qualitatively different. When there is no cell structure, D_x first increases, reaching a maximum very quickly at $t < 20\lambda_c/v$ and then decreases and follows the dotted $t^{-1/2}$ line closely, yielding the well known subdiffusion [2], [3]. This decrease is because most particles have by now traveled several parallel mean free paths so that in the parallel direction diffusion has set in. In stark contrast, when there is cell structure, however, the running diffusion coefficient D_x no longer follows $t^{-1/2}$ at $t > 20\lambda_c/v$. Instead, D_x at later times decreases and settles into a constant value, suggesting

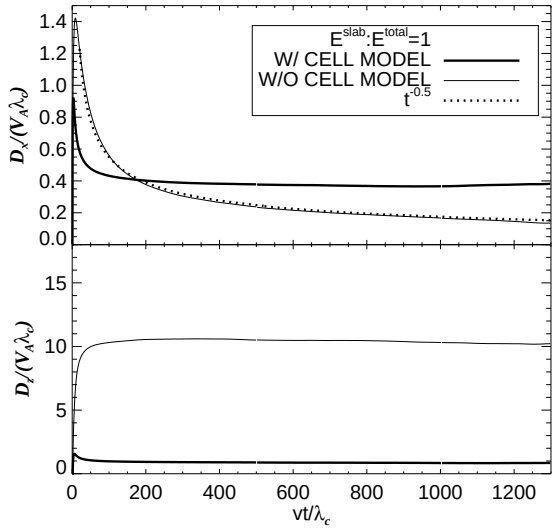

Fig. 2. Running perpendicular diffusion (upper panel) and running parallel diffusion (lower panel). Thick lines indicate local *intrinsic* pure slab turbulence with cell model. Thin lines indicate the same *intrinsic* turbulence without cell model. The *intrinsic* turbulence with or without cell model is pure slab with $r_L/\lambda_c = 0.098$ and $b/B_0 = 1.0$. Adapted from [21].

that a diffusion process in the perpendicular direction finally sets in.

This is a remarkable result. It suggest that, 2D structures such as current sheets, which do not fill up 3D solar wind, can nevertheless affect the intrinsic propagation properties of energetic particles. Clearly, to understand the transport of energetic particles in solar wind, one needs not only to specify the local geometry of a turbulence, but also need to specify some global properties (such as the existence of current sheets and its density, etc) of the turbulence. Having been often ignored before, this is however not a surprise: energetic particles often have much high energy than the background fluid, therefore they probe a much larger region comparing to fluid particles. As such, they will be able to probe various structures of fewer dimensions (in 2D) as they propagate. These fewer demension structures (including current sheets) are often where solar wind MHD turbulence intermittency manifest itself. Therefore, energetic particles can be effectively used as probes to study the intermittent characeristics of the solar wind MHD turbulence.

The transition from a sub-diffusion to a diffusion can be qualitatively understood as the following:

By dividing the solar wind into many cells and having the local background directions to be different in each cell, we are effectively forcing magnetic field lines to be twisted at the boundary. These twists require energy and can be regarded as effective turbulence powers. Because there is no correlation between the orientation of these boundaries with the background magnetic field, these power are not necessary in the parallel direction. Therefore, effectively we are generating turbulences of "2D" geometry. Consequently, particles will diffuse now instead of sub-diffuse.

Clearly the transition from sub-diffusion to diffusion should depend on the number density of current sheets in the solar wind and perhaps the ratio of b/B. Furthermore, it would be interesting to investigate how the power spectrum responds to the presence of current sheets. We plan to investigate these questions in the future.

IV. Conclusion

In the study of the transport of energetic particles in the solar wind, traditional approaches have been to assume that the magnetic field is composed of a uniform large scale background B_0 with a superposed δB. The turbulence field is often obtained by a Fourier transform of its spectrum $P(k)$, which is often prescribed globally in the whole 3D space. This picture ignores the presence of 2D structures that lead to intermittency to the solar wind MHD turbulence. Among these structures, current sheets are common. They can be generated in-situ or have a solar origin. Because magnetic field directions change rapidly on crossing a current sheet, it is crucial we include them when studying the transport of energetic particles. For example, these structures insured that diffusion to be a good approximation in both parallel and perpendicular directions to B_0. Further investigations on the effects of these structures should be carefully examined.

V. Acknowledgment

The author would like to thank Dr Yan Wang for stimulating discussions. This work was supported in part by NASA grants NNX06AC21G and NNH07ZDA001N.

References

[1] Parker, E. N., Planet. Space. Sci., 13, 9, 1965.
[2] Kóta, J. and Jokipii, J. R. 2000, *Astro. Phys. J.*, 531, 1067, 2000.
[3] Qin, G., Matthaeus, W. H., and Bieber, J. W. *Geophys. Res. Lett.*, 29(4), 1048, 2002a.
[4] Kolmogorov, A. N., *C. R. Acad. Sci. U.S.S.R.*, *30*, 301–305, 1941.
[5] Burlaga, L. F., *J. Geophys. Res.*, *96*, 5847–5851, 1991.
[6] Marsch, E., and S. Liu, *Ann. Geophysicae*, *11*, 227–238, 1993.
[7] Marsch, E., Tu, C.-Y., *Ann. Geophys.*. 12, 1127, 1994.
[8] Carbone, V., R. Bruno, and P. Veltri, in Lecture Notes in Physics, Vol. 462, 153–158, Springer-Verlag, 1995.
[9] Ruzmaikin, A. *et al.* , *J. Geophys. Res.*, *100*, 3395-3403, 1995.
[10] Tu, C.-Y., Marsch, E., *Ann. Geophys.*, 14, 270-285, 1996.
[11] Horbury, T. S. *et al.* , *Adv. Space Phys.*, *19*, 847–850, 1997.
[12] Bruno, R. *et al.* , *Geophys. Res. Lett.*, *26*, 3185–3188, 1999.
[13] Bruno, R. *et al.* , *Ann. Geophys., 22*, 3751, 2004.
[14] Veltri, P. *et al.* , *Nonlin. Proc. Geophys., 12*, 245, 2005.
[15] Salem, C., *et al.* , *AIP Conference Proceedings*, 932, 75-82, 2007.
[16] Li, G., *Astro. Phys. J. Lett., 672*, L65-68, 2008.
[17] Li, G., *AIP 932*, 26-31, 2007.
[18] Borovsky, J., 2006AGUFMSH43C05B, 2006.
[19] Chang, T. *et al.* , *Phys. Plasmas*, 11, 1287, 2004.
[20] Li, G., *et al.* , *Ann. Geophys.*, 26, 1889, 2008.
[21] Qin, G. and Li, G., *Astro. Phys. J. Lett.*, 682, L129, 2008.
[22] Matthaeus, W. H., *et al.* , *J. Geophys. Res.*, 95, 20673, 1990.
[23] Bieber, J. W., *et al.* , *J. Geophys. Res.*, 101, 2511, 1996.
[24] Qin, G., Matthaeus, W. H., and Bieber, J. W., *Astro. Phys. J.*, 578, L117, 2002b.